TRANSONIC FLUTTER/DIVERGENCE CHARACTERISTICS OF AEROELASTICALLY TAILORED AND NON-TAILORED HIGH-ASPECT-RATIO FORWARD SWEPT WINGS

Koji Isogai
National Aerospace Laboratory
Tokyo, Japan

Abstract

In order to see whether the divergence phenomenon of a transport type high-aspect-ratio forward swept wing can be effectively eliminated by aeroelastic tailoring, the experimental studies have been performed focusing attention especially on the transonic regime. The transonic flutter /divergence boundaries of the two wind tunnel models, one of which simulates the tailored full scale wing and the other of which simulates the non-tailored one, have been determined. The tailored model has experienced flutter as predicted by the linear theory which employs the Doublet Lattice Method. That is, the divergence phenomenon is suppressed by aeroelastic tailoring. The non-tailored model has experienced flutter contrary to the theoretical prediction, which is conjectured as "Shock Stall Flutter", in which the shock induced flow separation is playing the dominant role. By comparing the nondimensional flutter boundaries of the two models, it is shown that ,by aeroelastic tailoring, the transonic flutter characteristics of this particular wing can be improved about 60%-80% over that of the non-tailored wing.

1. Introduction

Divergence is a destructive aeroelastic phenomenon which is apt to occur especially for forward swept wings. This has long ruled out the practical use of forward swept wings, although they have several aerodynamic advantages compared with the conventional aft swept wings. However, the introduction of fibrous composites into the aircraft structures has been changing this situation. In early 1970s, Waddoups et al.[1] have first proposed an idea of controlling aeroelastic phenomena by positively utilizing the directional stiffness property of fibrous composites. This technology called "Aeroelastic Tailoring" has found its remarkable application in eliminating divergence, without increase of weight penalty, of forward swept wings. This has been first demonstrated by Krone[2] in 1974 in his design study using TSO(Tailoring and Structural Optimization Program)[3].

The wings he has studied are main wings of an executive jet transport and a light weight fighter, whose aspect ratios are moderate 4.0-5.0[2]. The Krone's conclusion has been extensively examined and proved theoretically and experimentally by many researchers in the course of the development of the X-29 forward swept wing demonstrator [4]. It is not, however, clear whether the aeroelastic tailoring is still effective for high-aspect-ratio transport type wings. Weisshaar[5] has examined theoretically the effect of aspect ratio on the divergence tailoring of forward swept wings ,concluding that the tailoring is still likely to be effective at fairly large aspect ratios. It is, however, to be noted that, in his study, the effects of tailoring on flutter of forward swept wings were not taken into account and the important transonic aerodynamic effects on the flutter/divergence characteristics of the forward swept wings were neglected also. Thus, in order to make his conclusion more confident, experimental verification should be pursued.

The purpose of the present study is to examine the effects of the aeroelastic tailoring on the transonic flutter and divergence characteristics of a transport type high-aspect-ratio forward swept wing. For this purpose, we have taken the following steps. In the first step, we have designed a tailored wing of a hypothetical transformer, which satisfies some given design requirements (static strength, flutter/divergence velocity). In addition to this tailored model, the non-tailored wing (therefore it is divergence critical) has also been designed for comparison purposes. Then, in the second step, we have designed and fabricated aeroelastically scaled models of these full scale wings and determined, experimentally, the aeroelastic characteristics of these models in the transonic tests. In the following sections, the detailed results of these analyses and experiments will be described.

2. Design and Analysis of a Full Scale Wing

In Fig. 1, the planform of the full scale wing of a hypothetical transformer of 150 seater, which we have studied in the first step, is shown. The aspect ratio of

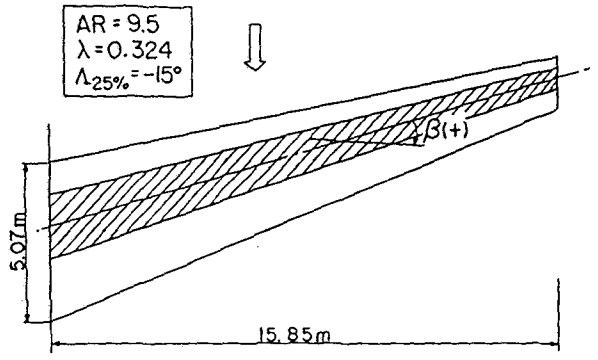

Fig. 1 Planform of full scale wing

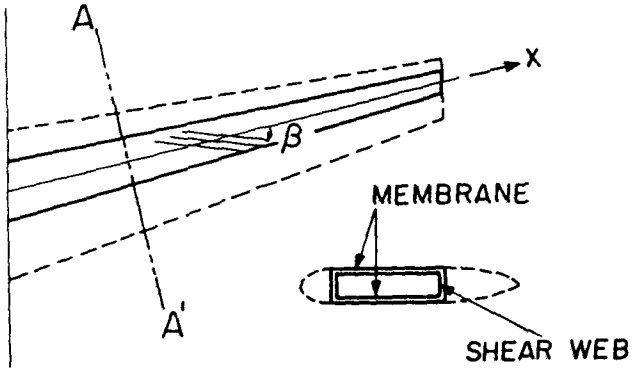

Fig. 2 Box beam model

the wing is 9.5 and the sweep angle of the quarter chord line is -15 degrees, and the taper ratio is 0.324. The wing has the natural laminar flow type supercritical airfoil sections of about 12% thick. The hatched part of the wing shows the location of the box beam. That is, the front and rear spars are located along the 20% and 60% chord lines, respectively. For this wing, we tentatively impose the following static strength and flutter/divergence velocity requirements.

a) It should sustain the static aerodynamic loading induced by the 2.5G flight condition, which corresponds with the loading of 794 KN acting on the semispan wing. (The load distribution induced at M =0.75, and α=2 deg is assumed)

b) The flutter/divergence velocity should clear 1.2 V_{max} (=306 m/s) (V_{max} is the design diving speed) at M =0.75 and altitude of 12,500 ft.

What we have to determine is the laminate construction of the upper and lower skin panels of the box structures, which satisfies the above design requirements.

In order to simplify the analysis it is assumed, as shown in Fig. 2, that the box beam is composed from the upper and lower membranes, and the front and rear shear webs. The laminate construction of the upper and lower membranes are assumed to be (β: 66%, 45°: 17%, -45°:17%)s, where β is the fiber orientation of the predominant layer, which is to be determined, by the parametric study, to meet the design requirements.

The parametric study has been done by using the preliminary design code developed at the National Aerospace Laboratory. The code is based on the beam theory[6] for the structural analysis and employes the unsteady lifting-surface theory (Doublet Lattice Method [7]) for the static and dynamic (flutter and divergence) aeroelastic analyses. The composite material used for this parametric study is the Graphite-Epoxy (T300/5208). The failure criterion used in the present study is that of Tsai-Wu[8] (the strength ratio R of the weakest layer should be greater than 1 under the 2.5G loading). The full fuel condition is assumed for determining the mass distribution. In Fig. 3, the results of the parametric study is shown. The thickness of the membrane is 12 mm at the root station and is tapered to the tip station with the taper ratio 0.324, and the same thickness distribution is also assumed for front and rear shear webs. In Fig. 3, the behaviors of the flutter velocity V_F and the divergence velocity V_D, the strength ratio R of the weakest layer, and the static aeroelastic deflection W_t and twist angle θ_t at the tip station are plotted with respect to the variation of the fiber orientation angle β. As seen in the figure, V_D, θ_t, and W_t are all very sensitive to the value of β,especially in the range between β=0° and -10°. That is,V_D increases rapidly as β varies from 0° to -10° without degradation of the flutter velocity. It also should be noted that the static aeroelastic deformations (θ_t and W_t) is very large for the values of β around 0° since the wing has the divergence tendency (although V_D still clears 1.2V_{max} = 306 m/s).

It is clear that β=-10° is the best choice for the design of this wing since V_F, V_D and R all satisfy the design requirements, and W_t and θ_t also stay in the reasonable range. The detailed quantitative results for the full scale wing, which are obtained for β=-10°, are as follows: The natural frequencies up to the sixth mode are 2.28 Hz, 7.78 Hz, 17.7 Hz, 20.8 Hz, 30.0 Hz, and 34.5 Hz, respectively. W_t and θ_t are 1.30 m (W_t/b_0=0.515) and θ_t =0.87°, respectively, where b_0 is the root semichord. The flutter/divergence conditions are as follows:

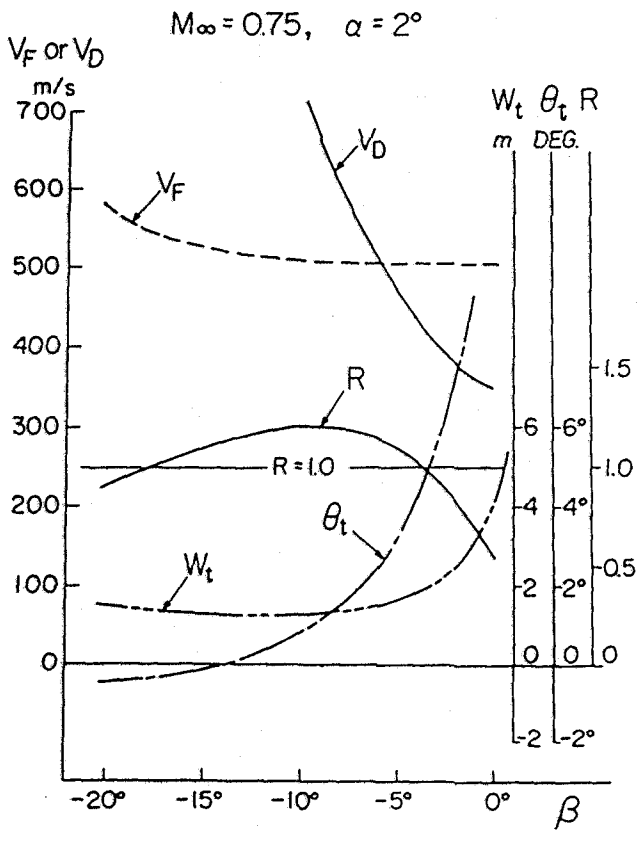

Fig. 3 Strength and aeroelastic characteristics of the full scale wing

V_F= 505.4 m/s, f_F = 6.83 Hz, k_F =0.215,
$\tilde{V}_F$ = 1.65, V_D = 826.3 m/s

where f_F is the flutter frequency, k_F is the reduced frequency and is defined by $(2\pi f_F b_0)/V_F$, and $\tilde{V}_F$ is defined by $\tilde{V}_F = V_F/(b_0\omega_1\sqrt{\mu})$ where ω_1 is the first natural frequency and μ is the mass ratio ($\mu = m/(\pi\rho\ b_0^2\ell\ (\lambda+(1-\lambda)^2/3))$, m: total mass of semispan (9,100 Kg), ℓ :semispan, ρ: air density, λ : taper ratio).

3. Evaluation by Wind-Tunnel Test

3.1 Design and Fabrication of Aeroelastic Scale Models

In order to confirm the results of the design study described in Sec. 2 for the main wing of the hypothetical transformer, we have designed and fabricated the aeroelastically scaled models of the full scale wing. The models are designed to confirm the flutter or divergence velocities of the full scale wing in the NAL 0.6 m x 0.6 m blow down transonic flutter wind tunnel. The planform and the construction of the wind tunnel models are shown in Fig. 4. As seen from Fig. 4, the model is constructed from the core composite beam and the urethane foam to provide the aerodynamic contours. It is a 1/45.5 scale model of the full scale wing, and is cantilever-mounted in the wind tunnel wall. As already mentioned in the previous section, we have designed two kinds of model, namely, the model which simulates the tailored wing (β= -10°) and the one which simulates the non-tailored wing (β= 0°). The laminate construction of the core composite beam of each model is determined so as to simulate the natural vibration characteristics of the corresponding full scale wing. As pointed out in Ref. 9, there is a simple relation

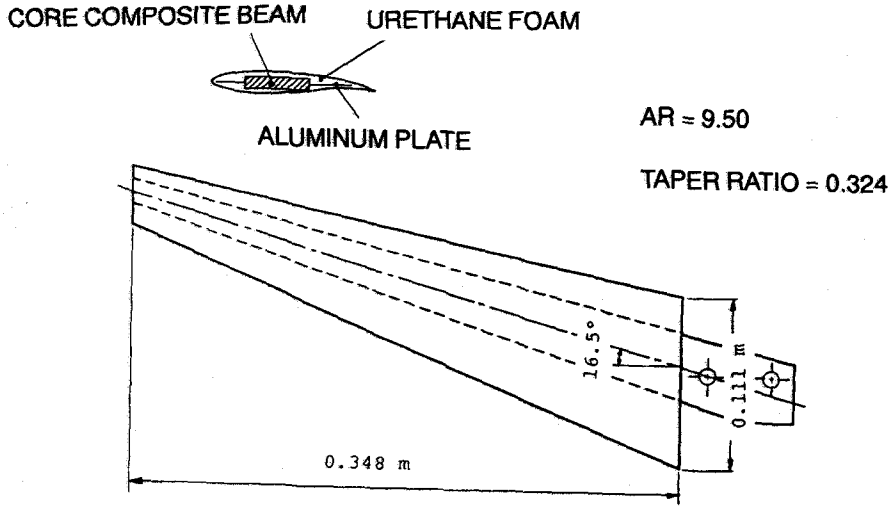

Fig. 4 Planform and construction of aeroelastically simulated wind tunnel model

between the laminate construction of upper (or lower) skin panel of the box structure and that of the solid beam, which approximately give the same vibration characteristics, if the effects of the front and rear spars of the box structure of the full scale wing are negligible. The relation presented in Ref. 9 is

$$h'_m \propto (h_B^2 h_m)^{1/3}$$

where h'_m, h_m and h_B are defined in Fig. 5, namely, h'_m is the distance to the upper edge of m th layer from the symmetry plane of the solid beam, while h_m is the distance to the upper edge of the m th layer from the symmetry plane of the upper/lower membrane of the box beam, and h_B is the distance between the symmetry planes of the upper and lower membranes of the box beam.

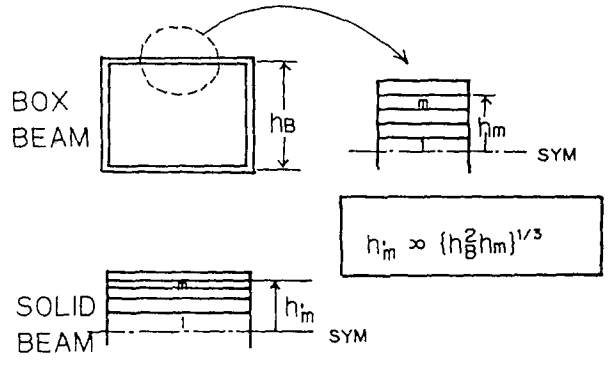

Fig. 5 Definition of laminate constructions of box skin panels and solid beam

By applying this relation, the laminate construction of the core composite beams of the models are determined as $(-10^o_{2.15}, 45^o_1, -45^o_{3.85})_s$ for the tailored model, which corresponds with the laminate construction, $(-10^o$:66%,45^o:17%, -45^o:17%$)_s$, of the skin panels of the full scale wing and as $(0^o_{2.15}, 45^o_1, -45^o_{3.85})_s$ for the non-tailored model, which corresponds with the laminate construction, $(0^o$:66%, 45^o:17%, -45^o:17%$)_s$, of the skin panels of the corresponding full scale wing. It is to be noted here that the subscript in the expressions of the laminate constructions of the core composite beams, which are given above, means the ratio of the thickness of each layer instead of meaning the number of plies, which is the usual definition. The thickness of the beam of the tailored model (Model A) is determined so that the hard flutter point is obtained in the operating range of our wind tunnel. The operating range of the NAL 0.6 m x 0.6 m Transonic Flutter Wind Tunnel is about 30.0 Kpa - 70 Kpa at M =0.60 and about 40 Kpa - 100 Kpa at M =0.80. The design point (hard flutter point of the tailored model) is set at about 62.5 Kpa at M =0.75. The thickness of the beam thus determined is 5.52 mm at the root station and 1.68 mm at the tip station. The beam is linearly tapered from the root to the tip station. The chordwise width of the beam is 40% of the local chord.

The thickness of the beam of the non-tailored model (Model B) is determined so that the (theoretical) divergence point is about 90.0 Kpa (at M =0.75) which is the upper limit of the tunnel operating range, since our intention is to determine the divergence boundary of the model by subcritical response technique (Southwell method [10],[11]). The thickness of the beam thus determined is 8.64 mm at the root station and 2.68 mm at the tip station.

The mass distributions of the models are determined by applying the aeroelastic similarity rule between the full scale wing and the scale models. The core composite beams of both models are fabricated by using the pre-pleg TOREKA T300/P3060B12. The measured elastic moduli of the material are E_L=130.0 Gpa, E_T=9.87 Gpa, ν_L=0.334, and G_{LT}=4.85 Gpa.

3.2 Natural Vibration Characteristics

The natural frequencies and mode shapes of each model were measured by the ground vibration test. The results are shown in Fig. 6a for the tailored model (Model A) and in Fig. 6b for the non-tailored model (Model B). The theoretical values of the natural frequencies and the node lines, which are calculated by the beam theory, are also shown in the same figures for comparison. The theoretical values of the natural frequencies shown in the figures are those calculated by adjusting the flexibility matrix so that the first natural frequency matches to that of the test. It should be noted that the distributions of the natural frequencies (f_n/f_1) and the nodal lines are in good agreement between the theory and the test for both the tailored and non-tailored models.

In order to see how well the wind tunnel model simulates the natural vibration characteristics of the hypothetical full scale wing, the distributions of the (experimental) natural frequencies and the node lines of the wind tunnel model and those (theoretical) of the full scale wing are also compared in Figs. 7a and 7b for the tailored and the non-tailored wings, respectively. As seen from the figures, the wind tunnel models well simulate the natural vibration characteristics of the full scale wings.

3.3 Test Results and Discussion

The flutter tests have been conducted in the 0.6 m x 0.6 m blow-down transonic wind tunnel of National Aerospace Laboratory. During the flutter tests, the dynamic pressure of the test section has been swept , with a specified (constant) Mach number, from low to

MODEL A (TAILORED) HZ

NATURAL FREQ.	f_1 (1B)	f_2 (2B)	f_3 (3B)	f_4 (1T)
	(f_1/f_1)	(f_2/f_1)	(f_3/f_1)	(f_4/f_1)
GROUND VIBRATION TEST	44.7 (1)	155.9 (3.49)	348.9 (7.80)	361.5 (8.09)
BEAM THEORY	44.7 (1)	152.0 (3.39)	343.3 (7.67)	366.1 (8.19)

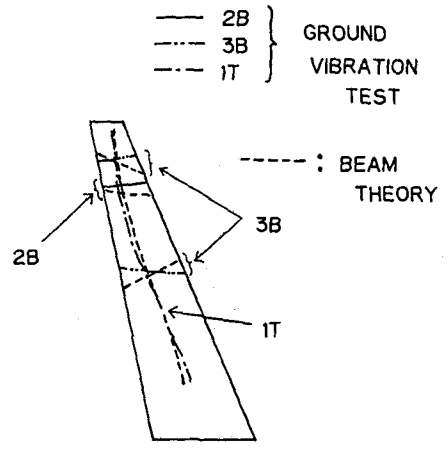

Fig. 6a Tailored model (Model A)
Natural frequencies and node lines of wind tunnel model

MOEL B (NON-TAILORED) HZ

NATURAL FREQ.	f_1 (1B)	f_2 (2B)	f_3 (1T)	f_4 (3B)
	(f_1/f_1)	(f_2/f_1)	(f_3/f_1)	(f_4/f_1)
GROUND VIBRATION TEST	80.7 (1)	304.0 (3.76)	549.0 (6.80)	657.0 (8.14)
BEAM THEORY	80.7 (1)	277.7 (3.44)	578.4 (7.17)	640.7 (7.94)

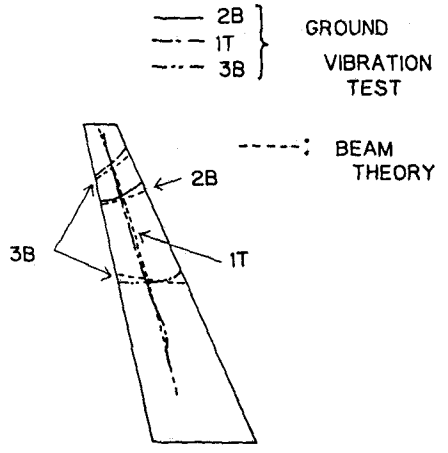

Fig. 6b Non-tailored model (Model B)
Natural frequencies and node lines of wind tunnel model

TAILORED WING HZ

NATURAL FREQ. / MODEL	f_1 (1B)	f_2 (2B)	f_3 (3B)	f_4 (1T)
	(f_1/f_1)	(f_2/f_1)	(f_3/f_1)	(f_4/f_1)
WIND TUNNEL MODEL	44.7 (1)	155.9 (3.49)	348.9 (7.80)	361.5 (8.09)
FULL SCALE WING	1.92 (1)	6.56 (3.42)	14.89 (7.76)	16.69 (8.69)

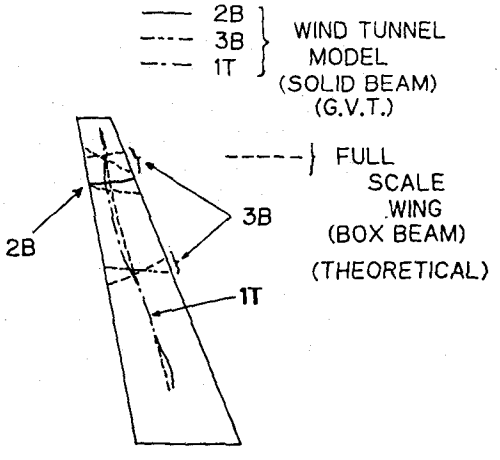

Fig. 7a Tailored wing
Comparison of natural frequencies and node lines between full scale wing and wind tunnel model

NON-TAILORED WING HZ

NATURAL FREQ. / MODEL	f_1 (1B)	f_2 (2B)	f_3 (1T)	f_4 (3B)
	(f_1/f_1)	(f_2/f_1)	(f_3/f_1)	(f_4/f_1)
WIND TUNNEL MODEL	80.7 (1)	304.0 (3.76)	549.0 (6.80)	657.0 (8.14)
FULL SCALE WING	2.14 (1)	7.33 (3.43)	15.57 (7.28)	16.83 (7.86)

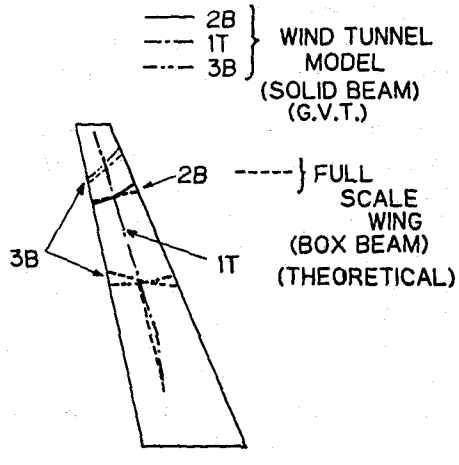

Fig. 7b Non-tailored wing
Comparison of natural frequencies and node lines between full scale wing and wind tunnel model

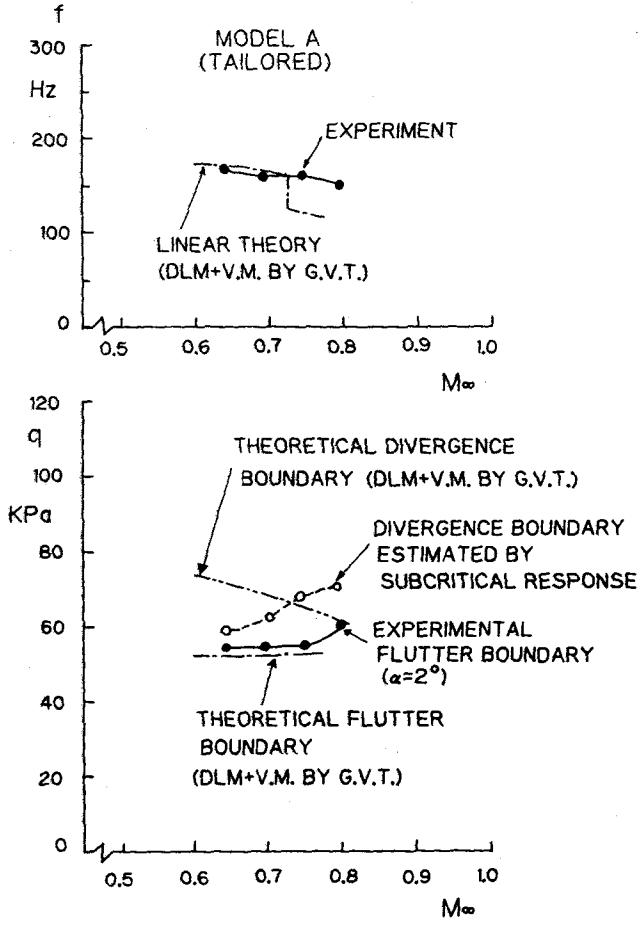

Fig. 8a Flutter dynamic pressure and frequency of tailored model

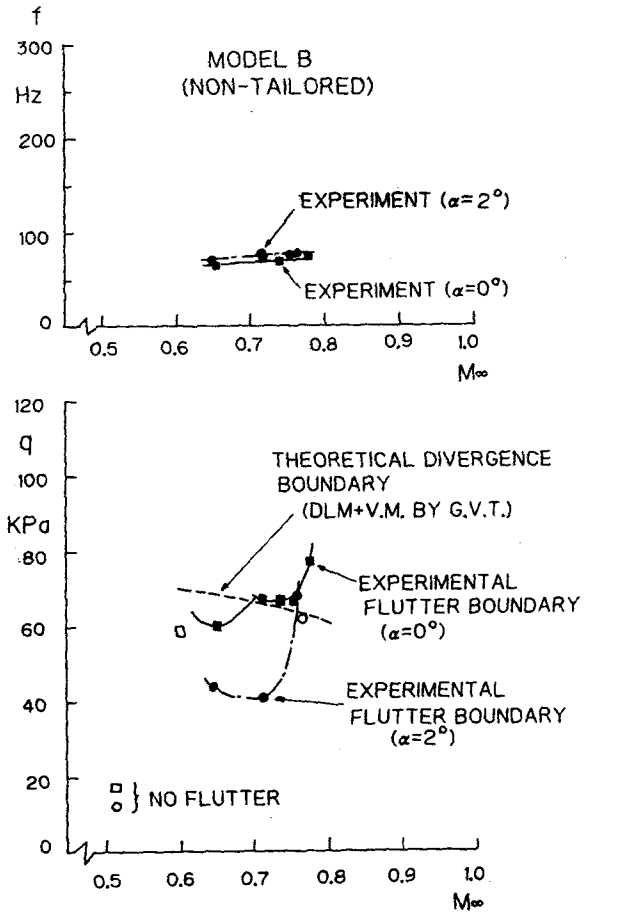

Fig. 8b Flutter dynamic pressure and frequency of non-tailored model

high values to obtain the hard flutter point. The strain guage signals from the models, which were obtained during sweeping the dynamic pressure, were recorded on the data recorder, having been used later for determining the hard flutter point and for the divergence point estimation by Southwell method.

In Fig. 8a, the experimental flutter boundary and frequencies of the tailored model (Model A) are plotted together with the divergence boundary estimated by Southwell method. The angle of attack of the model at the root station is 2° . The theoretical flutter and divergence boundaries of the model are also plotted in Fig. 8a for comparison. The theoretical values are obtained by employing the measured natural vibration modes and Doublet Lattice aerodynamics. As seen from the figure, the experimental flutter boundary is lower than the divergence boundary estimated by subcritical response data. This confirms the results of the design study described in Sec. 2. It is also interesting to see that the flutter boundary does not show the transonic dip phenomenon, which is commonly experienced for swept back wings with supercritical airfoil sections[12]. It is to be noted that the linear theory does a fairly good job for reproducing the experimental flutter boundary in this case.

In Fig. 8b, the experimental flutter boundaries and frequencies of the non-tailored model (Model B) , which are obtained for $\alpha=0^o$ and $\alpha=2^o$ respectively, are plotted together with the theoretical divergence boundary which are calculated by using measured natural vibration modes and Doublet Lattice aerodynamics. As shown in the figure and also discussed in Section 2, the theoretical prediction says that this non-tailored model should be divergence critical rather than flutter. However, what we have obtained in the experiment for this model is flutter rather than divergence as seen in Fig. 8b. This flutter phenomenon has two unusual characteristics compared with the conventional flutter such as experienced for model A. The first one is the flutter frequency. As seen in Fig. 8b, the flutter frequencies are about 64 Hz - 75 Hz depending on Mach numbers, which are slightly lower than the first natural frequency of this model (80.7 Hz). The second

characteristics is that the flutter boundary depends strongly on the mean angle of attack, that is, the flutter dynamic pressure decreases about 30% - 40% by changing the angle of attack from 0° to 2°. Further more, the divergence point estimated at M =0.73 and α_m =0° by Southwell method is about 145.1 Kpa which is far above the experimental flutter boundary and the theoretical divergence boundary shown in the figure. From those characteristics it is conjectured that the flutter experienced by this non-tailored model is "Shock Stall Flutter", in which the shock induced flow separation is playing the dominant role. It can easily be demonstrated that there is a mechanism of a single-degree-of-freedom flutter when the first natural mode shape of the wing has a wash-in tendency and the variation of the unsteady aerodynamic forces shows the hysteresis like that experienced for low speed stall flutter. Although, the law sped stall flutter only occurs at high angles of attack, the "Shock Stall Flutter" can occur even at low angles of attack since the non-tailored wing has a strong divergence tendency and the local angle of attack induced by the static aeroelastic deformation easily reaches the shock stall angle (which is the order of 5° - 6°), leading to the "Shock Stall Flutter". The very high divergence dynamic pressure estimated by the subcritical response technique seems to be attributed to the loss of the lift force due to the occurrence of the shock stall phenomenon. In order to validate these conjectures, further investigation should be pursued.

In order to see the improvement, by aeroelastic tailoring, of the aeroelastic characteristics of this forward swept wing, the dimensionless

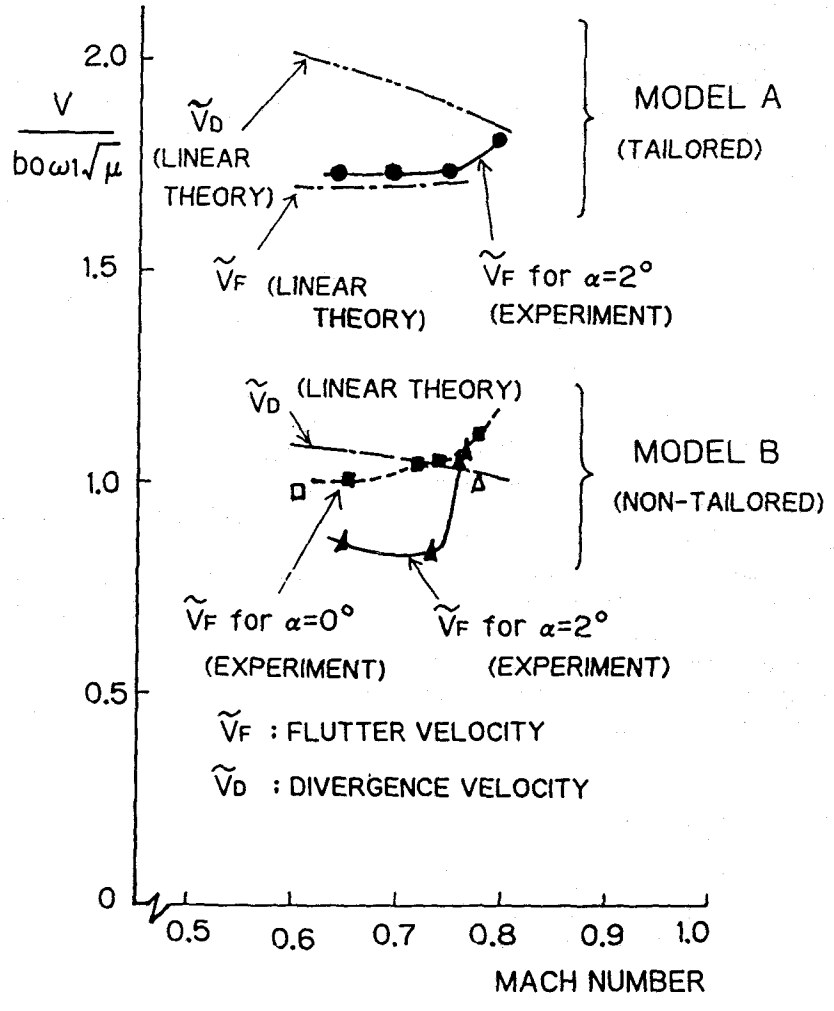

Fig. 9 Experimental and theoretical flutter/divergence characteristics of aeroelastically tailored and non-tailored high-aspect-ratio forward swept wings

flutter/divergence speeds of both the tailored and non-tailored models are plotted in the same figure, Fig. 9. As seen in the figure, by aeroelastic tailoring, we can eliminate divergence and improve the transonic flutter characteristics about 60% - 80% over that of the non-tailored wing.

4. Concluding Remarks

In order to see whether the divergence phenomenon of a transport type high-aspect-ratio forward swept wing can be effectively eliminated by aeroelastic tailoring, the experimental studies have been performed focusing attention especially on the transonic regime. The transonic flutter /divergence boundaries of the two wind tunnel models, one of which simulates the tailored full scale wing and the other of which simulates the non-tailored one, have been determined. The tailored model has experienced flutter as predicted by the linear theory which employs the Doublet Lattice Method. That is, the divergence phenomenon is suppressed by aeroelastic tailoring. The non-tailored model has experienced flutter contrary to the theoretical prediction, which is conjectured as "Shock Stall Flutter", in which the shock induced flow separation is playing the dominant role. By comparing the nondimensional flutter boundaries of the two models, it is shown that ,by aeroelastic tailoring, the transonic flutter characteristics of this particular wing can be improved about 60%-80% over that of the non-tailored wing.

Acknowledgement

The author is grateful to his colleagues Messrs. H. Ejiri, T. Kikuchi and J. Nakamichi for their supports in conducting flutter tests, and to Messrs. K. Yamane, I. Kumakura, T. Sotozaki and M. Minegishi for performing ground vibration tests, and to Mr. Y. Noguchi for measuring the elastic moduli of the composite material used for the wind tunnel models. He is also grateful to Drs. Kamiya and Onuki of the National Aerospace Laboratory for providing the planform and airfoil section data of the forward swept wing used in the present study.

References

1. Waddoups, M.E., Smith, C.B., and McMickle, R.W., "Composite Wing of Transonic Improvement, Composite Wing Aeroelastic Response Study," Air Force Flight Dynamics Lab., AFFDL-TR-71-24, Vol. I, Dec. 1972.

2. Krone, N.J.Jr.,"Divergence Elimination with Advanced Composites," Proc. of the AIAA 1975 Aircraft Systems and Technology Meeting, AIAA No. 75-1009, Aug. 1975.

3. McCullers, L.A., and Lynch, R.W.,"Dynamic Characteristics of Advanced Filamentary Composite Structure, Volume II- Aeroelastic Syntheses Procedure Development," Air Force Flight Dynamics Lab.,AFFDL-TR-73-111, Sept. 1974.

4. Hertz, T.J., Shirk, M.H., Ricketts, R.H., and Weisshaar, T.A.,"On the Track of Practical Forward-Swept Wings," Astronautics & Aeronautics, Jan. 1982, pp. 40-52.

5. Weisshaar, T.A.,"Aeroelastic Tailoring of Forward Swept Composite Wings," Journal of Aircraft, Vol. 18, No. 8, August 1981, pp. 669-676.

6. Austin, F., Hadcock, R., Hutchings, D., Sharp, D., Tang, S., and Waters, C., "Aeroelastic Tailoring of Advanced Composite Lifting-Surfaces in Preliminary Design," Proceedings of the AIAA/ASME/SAE 17th Structures, Structural Dynamics, and Materials Conference, May 1976, pp. 69-79.

7. Albano, E., and Rodden, W.P., "Doublet-Lattice Method for Calculating Lift Distributions on Oscillating Surfaces in Subsonic Flows," AIAA Journal, Vol., Feb. 1969, pp. 279-285.

8. Tsai, S.W., and Wu, E.M., "A General Theory of Strength for Anisotropic Materials, " Journal of Composite Materials, Vol. 5, Jan. 1971, pp. 58-80.

9. Isogai, K., "Some Problems of Aeroelasitc Scale Model of Aeroelastically Tailored Composite Wing," International Symposium on Scale Modeling, July 18-22, 1988, Tokyo, JSME, pp. 19-26.

10. Sherrer, V.C., Hertz, J.J., and Shirk, M.H., "Wind Tunnel Demonstration of Aeroelastic Tailoring Applied to Forward Swept Wings," Journal of Aircraft, AIAA 80-0796R, Vol. 18, No. 11, Nov. 1981, pp. 976-983.

11. Ricketts, R.H., and Doggett, R.V.Jr.,"Wind-Tunnel Experiments on Divergence of Forward-Swept Wings," NASA Technical Paper 1685, August 1980.

12. Farmer, M.G., and Hanson, P.W., "Comparison of Supercritical and Conventional Wing Flutter Characteristics," Proceedings, AIAA/ASME/SAE 17th Structures, Structural Dynamics and Materials Conference, King of Prussia, Pa., May 1976, pp. 608-614.